RESEARCH ARTICLE OPEN ACCESS

Artificial Neural Network Modeling for Dynamic Analysis of a Dam-Reservoir-Foundation System

Pr. Dr. Rafa H. S. Al-Suhaili[1], Pr. Dr. Ahmed A. M. Ali[2], Shamil A. K. Behaya[3]
[1]Prof. of Civil Engineering Dept., University of Baghdad, Baghdad, Iraq.
Visiting Prof. at The City College of New York, New York, USA.
[2]Prof. Water Resources Dept., Dean of the College of Engineering, University of Baghdad, Baghdad, Iraq.
[3]Assistant Lecturer University of Babylon, Babylon, Iraq.

Abstract

In this research, an Artificial Neural Networks (ANN) model is built and verified for quick estimation of the various maximum stresses, strains and hydrodynamic pressures developed on a gravity dam section due to seismic excitation. The developed model can be for accurate estimation of these values.

There are no explicit equations that relate the input to the output variables. It requires the solution of a system of simultaneous of partial differential equations governing the phenomenon, taking into account the three media interactions, dam body (concrete),reservoir(water) and foundation (soil).In this research a data base of 900 different cases inputs and outputs is build using the ANSYS software. Each of these input variables is assigned a range from which values are selected. These ranges were set according to the recommendations of authorized sources relevant to this issue. The statistical software SPSS with the database mentioned above are used, after converting the input and output variables to dimensionless forms, to build a model of Artificial Neural Networks ANN. The results showed the capability of the model to predict the values of the outputs (stresses and hydrodynamic pressures) with high accuracy. The correlation coefficients between the observed outputs values and the predicted values model are between 97.8% and 99.7%.The MATLAB programming language is used to write a program to apply the Artificial Neural Networks model for obtaining the stresses and hydrodynamic pressures for any set of input variables, instead of using the long process of ANSYS modeling. For the purpose of further checking of the performance of the model it was applied to a three different data cases which were not exist in the database that was used to build the model. The comparison of the results of these three cases obtained by the Artificial Neural Networks model with those obtained by using the ANSYS software had showed an excellent capability of the model to predict the outputs with high accuracy. The correlation coefficients for these three cases are 99.6%, 99.9% and 99.8% for the horizontal acceleration only, the vertical acceleration only and the dual acceleration (horizontal and vertical) respectively.

I. Introduction

Dams are man's oldest tools for storing water to sustain cities and irrigate the land for human survival. Today, some 45,000 dams around the world harness water for irrigation, domestic and industrial consumption, generation of electricity, and control of floods, *Veltrop (2002).*

Throughout the world insufficiencies have been observed in dams designed with consideration given to meteorological and hydrological data, which are stochastic in nature. The general importance of safety evaluations in dam engineering is explained in addition to the risk analysis that needs to be performed *,YenigunandErkek (2007).*

When it comes to safety, dams are critical structures that need careful consideration and accuracy during design and construction. On the other hand, economically, it is impossible to consider all safety issues. Therefore, to satisfy both economic and safety considerations simultaneously, an analysis should be conducted to select the better and more accurate method of design. One of the most critical safety cases is the behavior of the system under dynamic loading. The significant issue that is faced in predicting the behavior of dams and selecting the appropriate analytical model is the interaction of dams with water inside the reservoir, because the dynamic behavior of a structure in contact with water is different in that when this same structure is in contact with air, *Mansouri and Rezaei (2010)*.

An extensive stresses in the form of lateral inertial loads generate due to ground movements during seismic excitation on all types of structures. Also significant hydrodynamic pressure develops in additional to the hydrostatic pressure on the upstream faces of the dam from the water in the reservoir due to ground motions as well as movement of the structure in response to ground motions. The dam and the impounded water interact dynamically. Hydrodynamic pressure affects the deformation of dam which in turn influences the pressure. Frequency

and intensity of earthquake induced ground motion, depth of impounded reservoir, stiffness of structure and geological conditions are some of the factors affected the hydrodynamic response of dams.

Material properties and geometry of concrete gravity dam-reservoir-foundation systems as well as the seismic input along the dam axis are slightly varied therefore they are often idealized as two-dimensional sections in planes normal to the dam axis although they are three-dimensional.

In linear and non-linear dynamic analysis of concrete dams, the dam concrete and the foundation rock are modeled by standard finite elements, whereas the interaction effects of the impounded water can be represented by any of three basic approaches. The simplest one is the added mass attached to the dam, *Westergaard (1933).* Another approach describing the dam-water interaction is the Eulerian approach. In this approach, variables are displacements in the structure and pressures in the fluid, *Olsonet al. (1983).* Since these variables in the fluid and structure are different in this approach, a special-purpose computer program for the solution of coupled systems is required. The Lagrangian approach is a third way to represent the fluid-structure interaction. In this approach, behavior of fluid and structure are expressed in terms of displacements. Since available general-purpose structural analysis programs use the displacements to obtain the response of structures, Lagrangian displacement-based fluid elements can easily be incorporated into these programs, *Akkose and Simsek (2010).*

Dynamic interaction of dam-reservoir-foundation of concrete gravity dams is an important subject for researching on seismic performance of concrete gravity dams. Under earthquake, the response of concrete gravity dams becomes more complex because of the interaction of reservoir water and dams. Due to the dynamic interaction of dam-reservoir-foundation, the vibration energy is transferred and dispersion effect of earthquake excited is occurred under the influence of wave effect of inhomogeneous valley wall, *Xie et al. (2011).*

It seems to be necessary to select an appropriate numerical model, in the absent of any sufficient practical results. Many researchers worked on developing numerical models to evaluate seismic safety of concrete gravity dams in two and three-dimensional space, *Heirany and Ghaemian (2012).*

The first reported study approximately eighty years ago published by Westergaard clearly explained the physical behavior of the dam-reservoir interaction problem, *Westergaard (1933)*. Westergaard presented a conservative approximate equation for the hydrodynamic pressure distribution for a rigid dam. Continuing with the assumption that the gravity dam is rigid, *Chopra (1967)*suggested the more complete and comprehensive analyses formulas (the complex frequency response concept) for hydrodynamic pressure response of dam-reservoirs considering compressibility effects during harmonic and arbitrary horizontal as well as vertical components of ground motions. The same problem with more complete analysis including the effects of non-simultaneous arrival of seismic waves to the bottom of the reservoir was studied by*Victoria et al. (1969).*Extracting an analytical solution for the earthquake force on a rigid inclined upstream face of a dam by horizontal earthquakes first done by *Chwang and Housner (1978).*

Since that time researchers concentrated on identifying the influence of the incorrect properties and boundary conditions simplified assumptions, like rigid dam, rigid foundation, incompressible fluid, non-viscose fluid, no free surface waves in the reservoir and others on the hydrodynamic pressure and stresses on the dam body. *Bouaanani et al. (2003)*proposed a new approximate analytical technique for reliable estimate of hydrodynamic pressure on rigid gravity dams allowing for water compressibility and wave absorption at the reservoir bottom and can be extended to situations, such as the presence of an ice cover or gravity waves. *Navayineya et al. (2009)*then inspected the effect of fluid viscosity in frequency domain using a closed form solution. The effects of surface gravity waves on earthquake-induced hydrodynamic pressures on rigid dams with arbitrary upstream face are examined by *Aviles and Suarez (2010)*, taking the compressibility and viscosity of water into account. Also rigid dam with elastic reservoir bottom absorption of energy, subjected to a specified horizontal ground motion accelerogram was investigated by closed form formula, *Béjar (2010), Khiavi (2011).*

The finite element method has been widely used in seismic analysis of concrete gravity dams to analyze displacements and stresses in physical structures. Mathematically, the FEM is used for finding approximate solution of partial differential equations as well as of integral equations. The solution approach is based either on eliminating the differential equations completely, or rendering them into an equivalent ordinary differential equation. Although, there are different approaches available in this regard, the most natural method is based on the Lagrangian-Eulerian formulation, which employs nodal displacements and pressure degrees of freedom for the dam and reservoir region, respectively. Meanwhile, it is well known that in this formulation, the induced total mass and stiffness matrices of the coupled system are unsymmetrical due to interaction terms, *Zienkiewicz and Taylor (2000)*. *Shariatmadar and Mirhaj (2009)*evaluated the hydrodynamic pressures induced due to seismic forces and Fluid-

Structure Interaction (FSI).They used ANSYS computer program for modeling the interaction of reservoir water-dam structure and foundation bed rock and analyzed the modal response of over twenty 2D finite element models of concrete gravity dam. *Haciefendioglu et al. (2009)*presented numerical study concerning the dynamic response of a concrete dam including an ice covered reservoir. Non-linear seismic response of a concrete gravity dam subjected to near-fault and far-fault ground motions investigated by *Akkose and Simsek (2010)*including dam-water-sediment-foundation rock interaction.

Most engineers consider the water domain as a semi-infinite fluid region, while there are practical cases that the reservoir cannot be treated as a uniform infinite channel. *Fathi and Lotfi (2008)* shows that the length of the reservoir affects the response significantly and it should not be modeled as an infinite domain in general. Also *Bayraktar et al. (2010)*investigated the seismic performance of concrete gravity dams to near- and far-fault ground motions taking into account reservoir length variation. Because of the approximate concepts inherent in dam–reservoir interacting systems identification approaches, and the time-consuming repeated analyses required *Karimi et al. (2010)* employed the trained ANNs to investigate the potentialities of ANNs in system identification of gravity dams. A hybrid finite element–boundary element (FE–BE) analysis for the prediction of dynamic characteristics of an existing concrete gravity dam linked with an artificial neural network (ANN) procedure.

II. Theory of Dynamic Analysis

The dam-reservoir-foundation system can be classified as a coupled field system in which three physical domains of fluid, structure and soil interact only at their interfaces and these physical systems are made of subsystems which interact with each other. The time response of all subsystems must be evaluated at the same time due to the interaction in such a problem. There are different solutions approaches exist for the coupled field problem. The degrees of accuracy and stability of the solution depending on the governing differential equations of the subsystems and assumptions made for simplicity. The dam-reservoir-foundation system is three dimensional but is idealized as two dimensional sections in planes normal to the dam axis.

The dynamic equilibrium equation of interest is as follows for a linear structure:

$$[M]\{\ddot{u}\} + [C]\{\dot{u}\} + [K]\{u\} = \{F^a\} \quad (1)$$

where:[M] = structural mass matrix.
[C] = structural damping matrix.
[K] = structural stiffness matrix.
$\{\ddot{u}\}$ = nodal acceleration vector.
$\{\dot{u}\}$ = nodal velocity vector.
$\{u\}$ = nodal displacement vector.
$\{F^a\}$ = applied load vector.
$\{F^a\} = \{F^{nd}\} + \{F^e\}$ where:$\{F^{nd}\}$ = applied nodal load vector.
$\{F^e\}$=total of all element load vector effects.

In acoustical fluid-structure interaction problems, the structural dynamics equation needs to be considered along with the Navier-Stokes equations of fluid momentum and the flow continuity equation. The fluid momentum (Navier-Stokes) and continuity equations are simplified to get the acoustic wave equation using the following assumptions:

1. The fluid is compressible (density changes due to pressure variations).
2. The fluid is inviscid (no viscous dissipation).
3. There is no mean flow of the fluid.
4. The mean density and pressure are uniform throughout the fluid.

$$\frac{1}{C^2}\frac{\partial^2 P}{\partial t^2} - \nabla^2 P = 0 \quad (2)$$

where: C = speed of sound ($\sqrt{k/\rho_0}$) in fluid medium.
ρ_0 = mean fluid density.
k = bulk modulus of fluid.
P = acoustic pressure (=P(x, y, z, t)).
t = time.

Since the viscous dissipation has been neglected, Equation (2) is referred to as the lossless wave equation for propagation of sound in fluids. The discretized structural Equation (1) and the lossless wave Equation (2) have to be considered simultaneously in fluid-structure interaction problems.

For harmonically varying pressure, i.e.

$$P = \bar{P}e^{i\omega t} \quad (3)$$

where:$\overline{P}$ = amplitude of the pressure.

$i = \sqrt{-1}$.

$\omega = 2\pi f$.

f = frequency of oscillations of the pressure.

Equation (2) reduces to the Helmholtz equation:

$$\frac{\omega^2}{C^2}\overline{P} + \nabla^2\overline{P} = 0 \quad (4)$$

The acoustics fluid equation can be written in matrix notation to get the discretized wave equation:

$$[M_e^p]\{\ddot{P}_e\} + [K_e^p]\{P_e\} + \rho_0[R_e]^T\{\ddot{u}_e\} = \{0\} \quad (5)$$

where:$[M_e^p] = \frac{1}{C^2}\int_{vol}\{N\}\{N\}^T\, d(vol)$ = fluid mass matrix (fluid).

$[K_e^p] = \int_{vol}[B]^T[B]\, d(vol)$ = fluid stiffness matrix (fluid).

$\rho_0[R_e]^T = \rho_0 \int_S \{N\}\{n\}^T\{N'\}^T\, d(S)$ = coupling mass matrix transpose (fluid-structure interface).

To account for the dissipation of energy due to damping at the boundary, if any, present at the fluid boundary, a dissipation term is added to the lossless equation to get finally the discretized wave equation accounting for losses at the interface as:

$$[M_e^p]\{\ddot{P}_e\} + [C_e^p]\{\dot{P}_e\} + [K_e^p]\{P_e\} + \rho_0[R_e]^T\{\ddot{u}_e\} = 0 \quad (6)$$

In order to completely describe the fluid-structure interaction problem, the fluid pressure load acting at the interface is now added to Equation (1). So, the structural equation is rewritten here:

$$[M_e]\{\ddot{u}_e\} + [C_e]\{\dot{u}_e\} + [K_e]\{u_e\} = \{F_e\} + \{F_e^{pr}\} \quad (7)$$

The substitution of $\{F_e^{pr}\} = [R_e]\{P_e\}$, where$[R_e]^T = \int_S \{N'\}\{N\}^T\{n\}d(S)$, into Equation (7) results in the dynamic elemental equation of the structure:

$$[M_e]\{\ddot{u}_e\} + [C_e]\{\dot{u}_e\} + [K_e]\{u_e\} - [R_e]\{P_e\} = \{F_e\} \quad (8)$$

Equation (6) and Equation (8) describe the complete finite element discretized equations for the fluid-structure traction problem and are written in assembled form as:

$$\begin{bmatrix}[M_e] & [0]\\ [M^{fs}] & [M_e^p]\end{bmatrix}\begin{Bmatrix}\{\ddot{u}_e\}\\ \{\ddot{P}_e\}\end{Bmatrix} + \begin{bmatrix}[C_e] & [0]\\ [0] & [C_e^p]\end{bmatrix}\begin{Bmatrix}\{\dot{u}_e\}\\ \{\dot{P}_e\}\end{Bmatrix} + \begin{bmatrix}[K_e] & [K^{fs}]\\ [0] & [K_e^p]\end{bmatrix}\begin{Bmatrix}\{u_e\}\\ \{P_e\}\end{Bmatrix} = \begin{Bmatrix}\{F_e\}\\ \{0\}\end{Bmatrix} \quad (9)$$

where: $[M^{fs}] = \rho_0[R_e]^T$

$[K^{fs}] = -[R_e]$

III. Harmonic Response Analysis

The harmonic response analysis solves the time-dependent equations of motion (Equation 2) for linear structures undergoing steady-state vibration. The assumptions and restrictions are:

1. Valid for structural and fluid degrees of freedom (DOFs).
2. The entire structure has constant or frequency-dependent stiffness, damping, and mass effects.
3. All loads and displacements vary in sinusoidal way at the same known frequency (although not necessarily in phase).
4. Element loads are assumed to be real (in-phase) only.

As stated above, all points in the structure are moving at the same known frequency, however, not necessarily in phase. Also, it is known that the presence of damping causes phase shifts. Therefore, the displacements may be defined as:

$$\{u\} = \{u_{max}\, e^{i\emptyset}\}e^{i\Omega t} \quad (10)$$

where: u_{max} = maximum displacement.

i = square root of -1.

Ω= imposed circular frequency (radians/time) = $2\pi f$.

f = imposed frequency (cycles/time).

t = time.

∅ = displacement phase shift (radians).

Note that u_{max} and ∅ may be different at each DOF. The use of complex notation allows a compact and efficient description and solution of the problem. Equation (10) can be rewritten as:

$$\{u\} = \{u_{max}\,(\cos\emptyset + i\sin\emptyset)\}e^{i\Omega t} \quad (11)$$

Or as:$\{u\} = (\{u_1\} + i\{u_2\})e^{i\Omega t}$ (12)

where:$\{u_1\} = u_{max}\cos\emptyset$ = real displacement vector.

$\{u_2\} = u_{max}\sin\emptyset$ = imaginary displacement vector.

The force vector can be specified analogously to the displacement:

$$\{F\} = \{F_{max}\, e^{i\varphi}\}e^{i\Omega t} \quad (13)$$
$$\{F\} = \{F_{max}\,(\cos\varphi + i\sin\varphi)\}e^{i\Omega t} \quad (14)$$
$$\{F\} = (\{F_1\} + i\{F_2\})e^{i\Omega t} \quad (15)$$

where: F_{max} = force amplitude.
φ = force phase shift (radians).
$\{F_1\} = \{F_{max}\cos\varphi\}$ = real force vector.
$\{F_2\} = \{F_{max}\sin\varphi\}$ = imaginary force vector.

Substituting Equation (12) and Equation (15) into Equation (1) gives:

$$([K] - \Omega^2[M] + i\Omega[C])(\{u_1\} + i\{u_2\}) = \{F_1\} + i\{F_2\} \quad (16)$$

The complex displacement output at each DOF may be given in one of two forms:

1. The same form as u_1 and u_2 as defined in equation (12).
2. The form u_{max} and $\emptyset$ (amplitude and phase angle (in degrees)), as defined in equation (11). These two terms are computed at each DOF as:

$$u_{max} = \sqrt{u_1^2 + u_2^2} \quad (17)$$
$$\emptyset = \tan^{-1}\frac{u_2}{u_1} \quad (18)$$

Note that the response lags the excitation by a phase angle of $\emptyset - \varphi$.

Inertia, damping and static loads on the nodes of each element are computed. The real and imaginary inertia load parts of the element output are computed by:

$$\{F_1^m\}_e = \Omega^2[M_e]\{u_1\}_e \quad (19)$$
$$\{F_2^m\}_e = \Omega^2[M_e]\{u_2\}_e \quad (20)$$

Where: $\{F_1^m\}_e$ = vector of element inertia forces (real part).
$[M_e]$ = element mass matrix.
$\{u_1\}_e$ = element real displacement vector.
$\{F_2^m\}_e$ = vector of element inertia (imaginary part).
$\{u_2\}_e$ = element imaginary displacement vector.

The real and imaginary damping loads parts of the element output are computed by:

$$\{F_1^C\}_e = -\Omega[C_e]\{u_2\}_e \quad (21)$$
$$\{F_2^C\}_e = \Omega[C_e]\{u_1\}_e \quad (22)$$

Where: $\{F_1^C\}_e$ = vector of element damping forces (real part).
$[C_e]$ = element damping matrix.
$\{F_2^C\}_e$ = vector of element damping (imaginary part).

The real static load is computed the same way as in a static analysis using the real part of the displacement solution $\{u_1\}_e$. The imaginary static load is computed also the same way, using the imaginary part $\{u_2\}_e$. Note that the imaginary part of the element loads (e.g., $\{F^{pr}\}$) are normally zero, except for current density loads.

The nodal reaction loads are computed as the sum of all three types of loads (inertia, damping, and static) over all elements connected to a given fixed displacement node.

IV. Research Procedures

The following steps are conducted in this research to develop the ANN model:

1- Building a data base for different cases, i.e. different sets of input-output variables using the ANSYS12.1 (2009) software. The input variables are selected according to the limitations of dam section variables given in dam design recommendation references.
2- Obtain a direct relationship between the selected sets of input variables and the obtained output variables in dimensionless forms using Artificial Neural Network Model using the IBM SPSS statistics 19 (2010) software. This allows two simple matrices equations that enable the estimation of output variables for a given set of input variables.
3- The model developed in step (2) is verified using comparison of results obtained from the ANN model and these obtained from ANSYS analysis, using some selected cases not included in the data base developed in step (1) above. The MATLAB programming language is used to develop a program using the developed ANN model for analysis. This verification process is done to ensure the capability of the ANN model to produce acceptable results, even though the ANN model processing divide the data set into three sub-division, training, testing and holdout (verification) subset, and evaluate the performance of the model using the third set, which is not used for model parameters estimation.

V. ANSYS Application

The system to be analyzed is a concrete gravity dam which impounds a reservoir extending to truncation line in the upstream direction and rests on a bounded foundation. General schematic section geometry of the dam is shown in Figure (1) below:

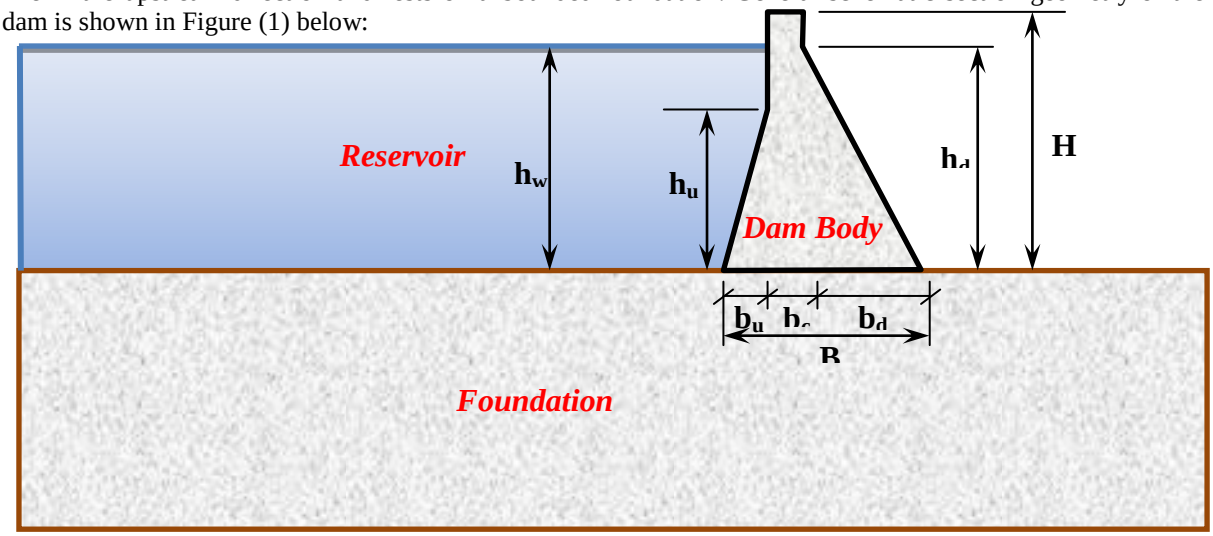

Fig. 1: Schematic presentation of the dam-reservoir-foundation system analyzed dynamically using ANSYS.

where: H: total dam height, B: total dam base width, h_w: water height in the reservoir, b_u: upstream dam face slope width, h_u: upstream dam face slope height, b_c: dam crest width, h_d: downstream dam back slope height and b_d: downstream dam back slope width.

The dynamic analysis needs to identify other variables in addition to those geometric variables presented in Figure (1). These variables can be categorized into three groups as follows:

1- Geometric variables: concerning the section details.
2- Properties variables: concerning domains properties such as modulus of elasticity, density, Poisson's ratio…etc., of the three domains coupled (water, concrete dam body and soil foundation).
3- Excitation variables: concerning the excitation earthquake variables such as accelerations and frequencies.

In order to obtain a general ANN model, the variables should be put in non-dimensional forms. This is conducted as follows, with the range of each non-dimensional variable limitation. These limitations were decided upon the limitations of the dam design practice and recommendations to satisfy stability and overturning control, *Novak et.al. (2007), EM 1110-2-2200 (1995), Chahar (2013), WikipediaEncyclopedia (2013).*

Table (1) shows the dimensionless variables that were adopted to build a database for the cases analyzed using ANSYS software for the dynamic response of the couple dam-reservoir-foundation system.

Table 1: Dimensionless input variables selected for dynamic analysis of dam-reservoir-foundation system.

Variables Ratio	Range	Values Adopted		
B/H	0.70 - 0.80	0.70	0.75	0.80
h_w/H	0.85 - 0.95	0.85	0.90	0.95
h_u/H	0.50 - 0.70	0.50	0.60	0.70
h_d/H	0.80 - 0.90	0.80	0.85	0.90
b_u/B	0.07 - 0.08	0.07	0.075	0.08
b_c/B	0.09 - 0.14	0.09	0.12	0.14
b_d/B	0.788 - 0.84	0.788	0.80	0.84
a_x/g	0.10 - 0.30	0.10	0.20	0.30
a_y/g	0.05 - 0.25	0.05	0.15	0.25

w/w_n	0.50 - 1.10	0.50	0.80	1.10
E_s/E_c	0.50 – 2.00	0.50	1.00	2.00
ρ_s/ρ_c	0.875 - 1.125	0.875	1.00	1.125

Natural frequency for the dam-reservoir-foundation system is computed according to the empirical relations proposed by Chopra shown in Table (2), *Chopra and Charles (1979)*.The output variables from the ANSYS analysis (stresses and hydrodynamic pressure) are changed also to dimensionless quantities by dividing each by its respective allowable values for the dam body, and by the hydrostatic pressure values for the hydrodynamic pressure.

Table 2: Natural frequency for the dam-reservoir-foundation system.

Soil-Concrete Elasticity Ratio (E_s/E_c)	**Reservoir Depth (h_w) in (m)**					
	85		**90**		**95**	
	Natural Frequency (w_n) in (Hz)					
	By Chopra	**By ANSYS**	**By Chopra**	**By ANSYS**	**By Chopra**	**By ANSYS**
0.5	2.473	2.448	2.370	2.474	2.232	2.384
1	3.175	2.899	3.040	2.913	2.874	2.769
2	3.353	3.220	3.215	3.215	3.030	3.204

VI. Boundary Conditions

The boundary conditions used for the dam-reservoir-foundation system in the ANSYS analysis are shown in Figure (2) bellow.

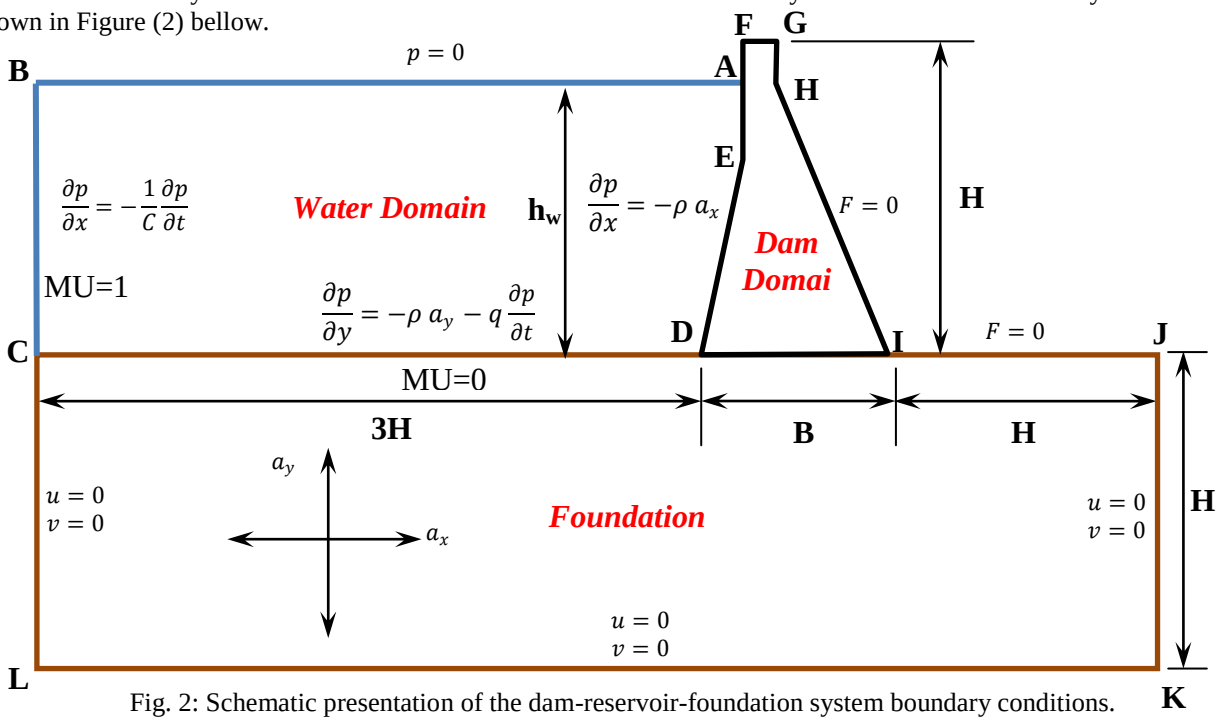

Fig. 2: Schematic presentation of the dam-reservoir-foundation system boundary conditions.

VII. Materials Properties

The concrete is assumed homogeneous and isotropic, the water is considered as compressible, inviscid fluid and the dam-foundation treated as homogeneous and isotropic. Table (3) shows the dam-reservoir-foundation system properties.

Table 3: The dam-reservoir-foundation system properties.

Modulus of Elasticity (*E*) *GPa*	**Mass Density (ρ) kg/m^3**	**Poisson's Ratio *v***	**Damping Coefficient *q***	**Velocity of Sound Wave *(C) m/s***
Water in the Reservoir				
2.07*	1000	0.49	MU=1	1440
Concrete of the Dam				
25	2400	0.2	0.05	-
Soil of the Foundation				
12.5	2100	0.3	0.05	-
25	2400			
50	2700			

*Bulk Modulus of Elasticity (Compressibility).

VIII. Element Used in ANSYS Analysis

The "plane Strain" state is governing on the cross section of dam, because of the longitudinal length is very greater than other two dimensions, *EM 1110-2-6051 (2003)*. Hence, two-dimensional finite element models are created. The elements used for ANSYS analysis are as follows:

1- "FLUID 29" element: This is four nodes 2-D element with one degree of freedom (1DOF) for pressure, suitable for model acoustic fluid for modeling water of reservoir, with the options of the structure present and structure absent. For structure present elements, each node has three degree of freedom (3DOF), which account for water particles displacement in horizontal and vertical direction and pressure.
2- "PLANE 42" element: This is used for modeling both concrete dam body and foundation bed soil. This 2-D plane element has four nodes with two degrees of freedom (2DOF) for each, which account for solid particles horizontal and vertical displacement.
3- "CONTA 171" element: This element is adopted for the interface surface between two different domain, fluid and solid elements.
4- "TARGE 169" element: This element is adopted for the interface surface between two solid domains with different properties, concrete dam and soil elements.

IX. Results of ANSYS Application

The ANSYS software used to find the dynamic response of given dam-reservoir-foundation system to a dynamic loading (earthquake), to build the database required for the ANN model. The harmonic analysis is used to predict this response, i.e. transforming the governing equation from time domain to frequency domain. This allows obtaining the maximum amplitude of hydrodynamic pressure, hence, maximum dynamic forces applied to the system. Nine hundred cases selected due for variation of the dimensionless input variables that covers the variations shown in Table (1).

For results, presentation purposes one case of vertical and horizontal accelerations is selected. The details of input variables are shows on Table (4).As the ANSYS capabilities of graphical representation of the result are excellent, the graphical presentations of the results are shows in Figures (8) to (21) for the selected case.

Table 4: The selected case variables.

Input Variables	**B/H**	**h_w/H**	**h_u/H**	**h_d/H**	**b_u/B**	**b_c/B**	**b_d/B**	**a_x/g**	**a_y/g**	**w/w_n**	**E_s/E_c**	**ρ_s/ρ_c**
Value	0.80	0.90	0.70	0.85	0.09	0.11	0.80	0.20	0.15	0.50 1.10	0.50	0.88

Figures (3) to (6) shows the natural frequency modes (modes 1 to 4) which indicates that the mode (1) natural frequency is (2.474). Mode (2) natural frequency is (3.512). Mode (3) frequency is (4.038). Mode (4) frequency is (4.504).

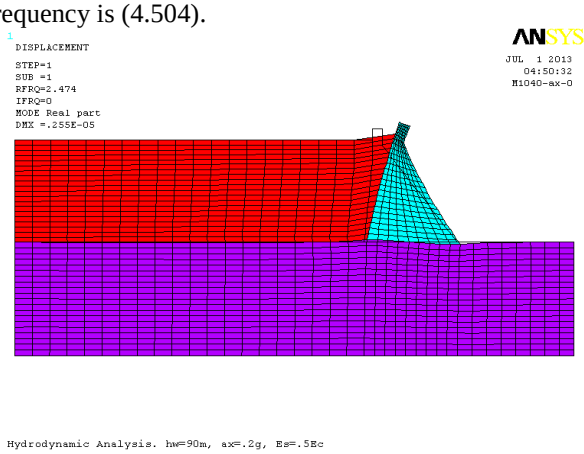

Fig. 3: Natural Frequency Mode 1.

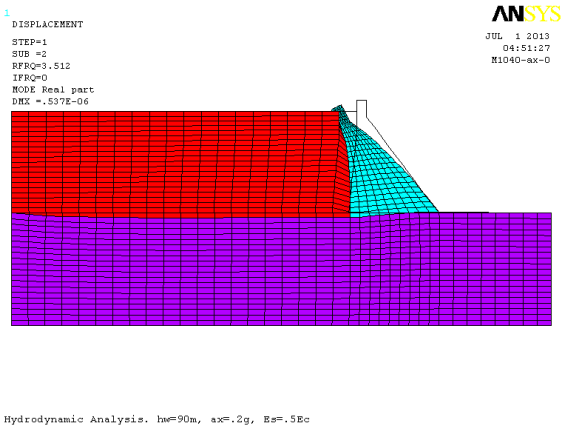

Fig. 4: Natural Frequency Mode 2.

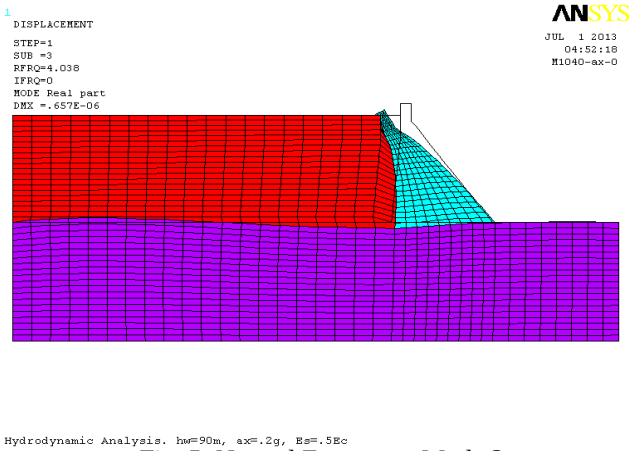

Fig. 5: Natural Frequency Mode 3.

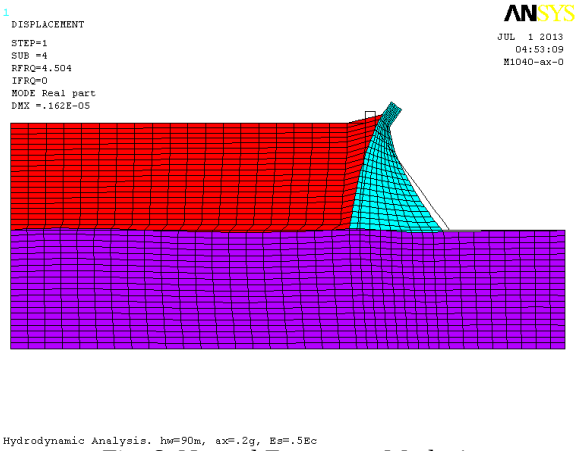

Fig. 6: Natural Frequency Mode 4.

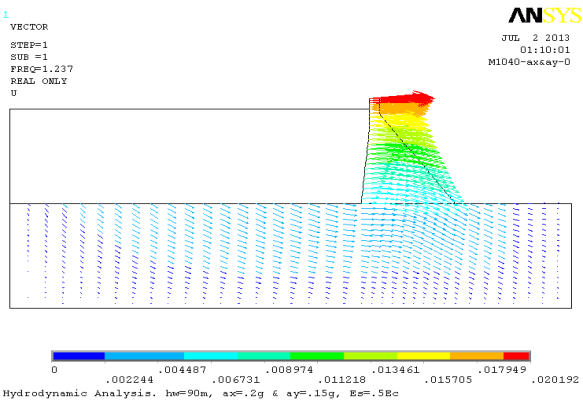

Fig. 8: Displacement Vectors for Case (Hor. & Ver. Acceleration)w/w_n=0.5.

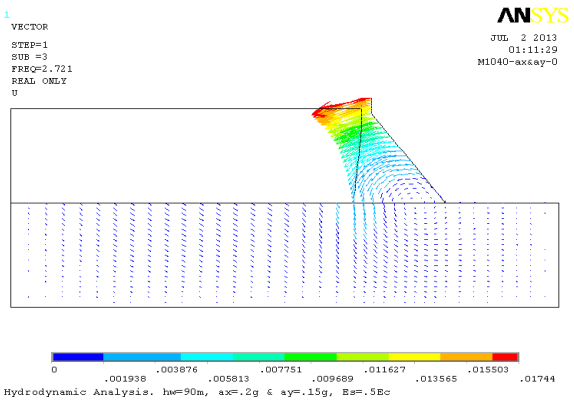

Fig. 9: Displacement Vectors for Case (Hor. & Ver. Acceleration)w/w_n=1.1.

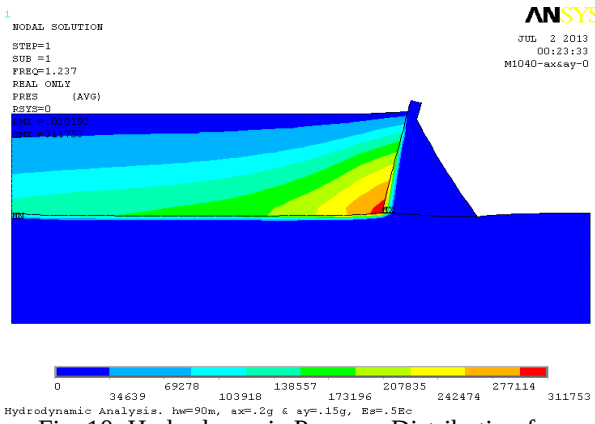

Fig. 10: Hydrodynamic Pressure Distribution for w/w_n= 0.5

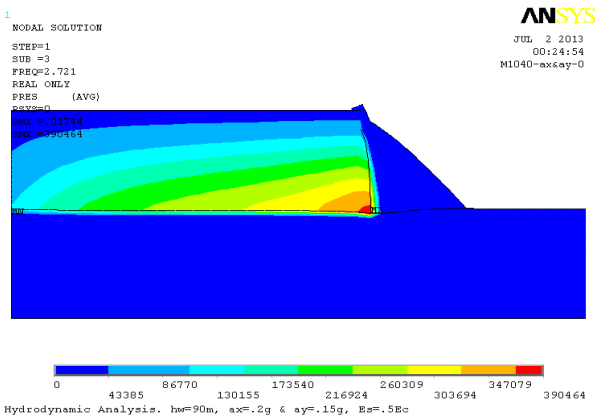

Fig. 11: Hydrodynamic Pressure Distribution for w/w_n= 1.1.

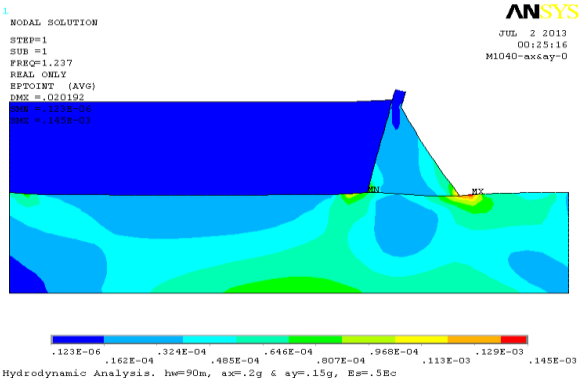

Fig. 12: Strain Intensity for w/w_n= 0.5.

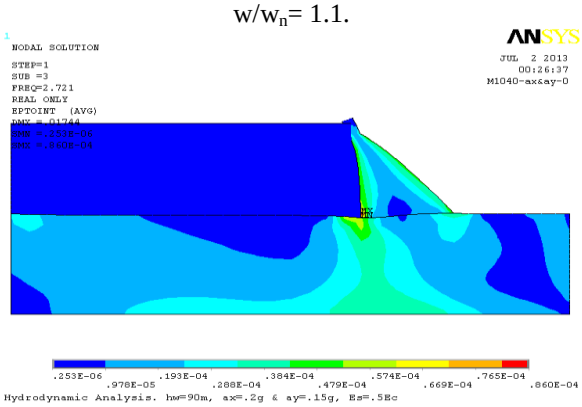

Fig. 13: Strain Intensity for w/w_n= 1.1.

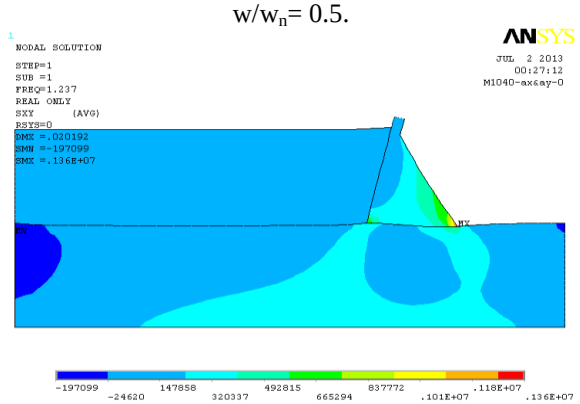

Fig. 14: Shear Stress Intensity for w/w_n= 0.5.

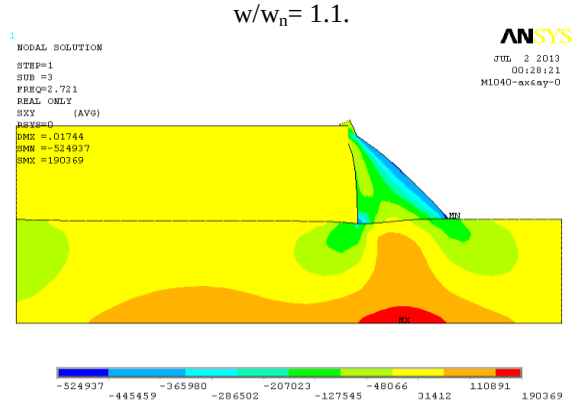

Fig. 15: Shear Stress Intensity for w/w_n= 1.1.

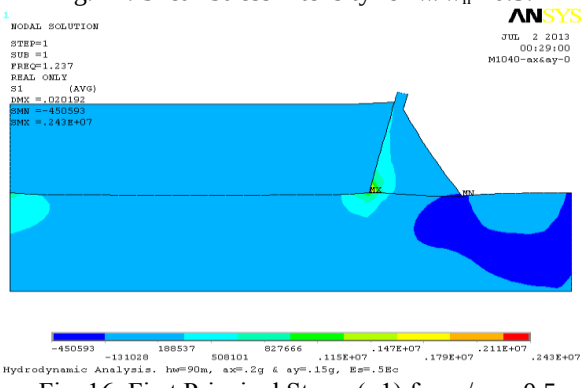

Fig. 16: First Principal Stress (σ1) for w/w_n= 0.5.

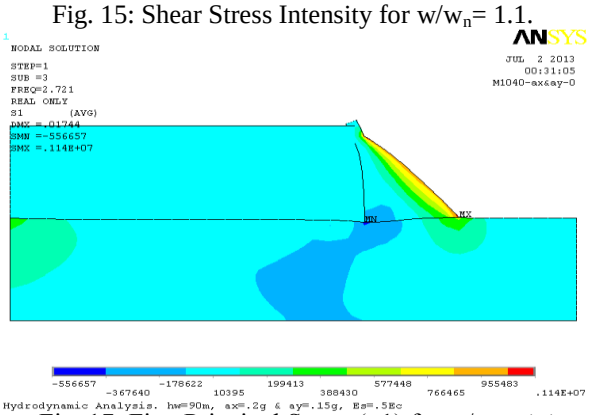

Fig. 17: First Principal Stress (σ1) for w/w_n= 1.1.

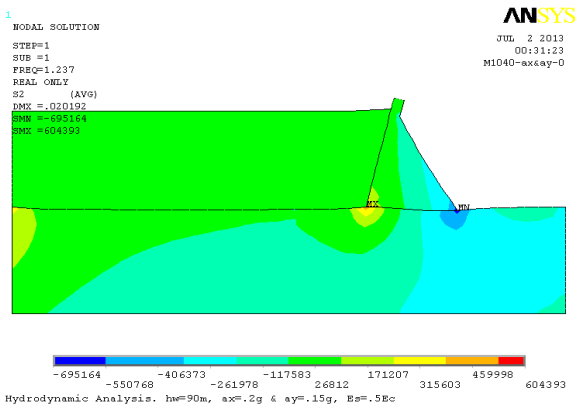

Fig. 18: Second Principal Stress (σ2) for w/w_n= 0.5.

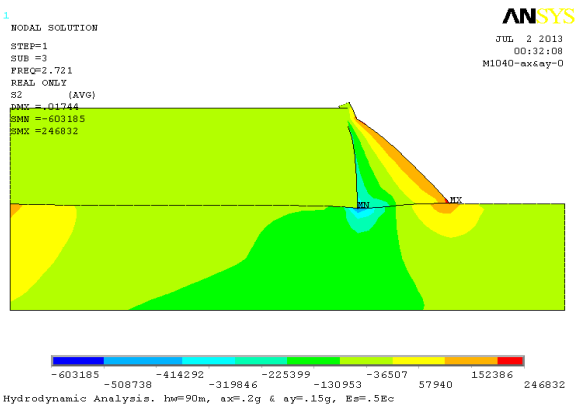

Fig. 19: Second Principal Stress (σ2) for w/w_n= 1.1.

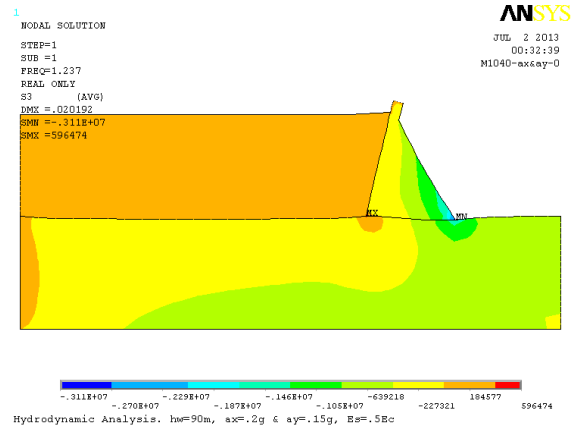

Fig. 20: Third Principal Stress (σ3) for w/w_n= 0.5.

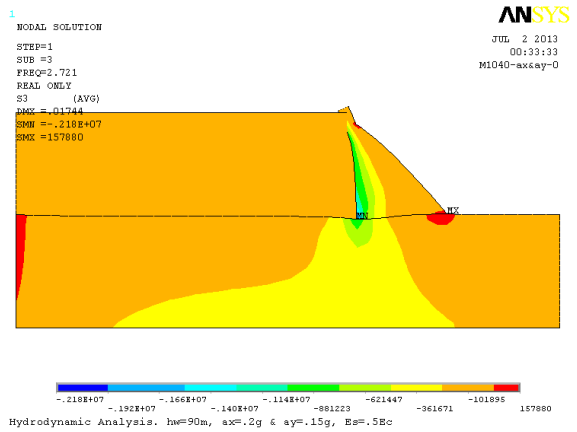

Fig. 21: Third Principal Stress (σ3) for w/w_n= 1.1.

The ANN Model

A direct relation could be obtained using an ANN model, which needs a database of the set of output variables related to the respective input variables. These variables are set in dimensionless terms as given by Table (1) to obtain a general relationship model.

The IBM SPSS statistics 19 (2010) "Statistical Product and Service Solutions" software is used with the developed database to obtain the parameters matrices and vectors of this ANN model $(v_{o_{p\times1}}, v_{n\times p}, w_{o_{m\times1}}, w_{p\times m})$.

The standardization process is used here for the modeling process, hence, the mean and standard deviation values of each variable (input and output), will become a set of model parameters in addition to the weight matrices and bias vectors $(v_{n\times p}, w_{p\times m}, v_{o_{p\times1}}, w_{o_{m\times1}})$. Table (5) shows this values obtained using SPSS software.

Table 5: mean and standard deviation values.

Variable Type	*Variable Name*	*Min.*	*Max.*	*Mean*	*Std. Deviation*	*Variance*
Inputs	B/H	.7500	.8500	.796833	.0404160	.002
	h_w/H	.8500	.9500	.896500	.0418094	.002
	h_u/H	.5000	.7000	.591333	.0816433	.007
	h_d/H	.8000	.9000	.858333	.0412203	.002
	b_u/B	.0630	.0880	.074537	.0091251	.000

Variable Type	***Variable Name***	***Min.***	***Max.***	***Mean***	***Std. Deviation***	***Variance***
	b_c/B	.0930	.1500	.114783	.0197512	.000
	b_d/B	.7880	.8400	.811080	.0219127	.000
	a_x/g	.0000	.3000	.130000	.1168268	.014
	a_y/g	.0000	.2500	.096833	.0968266	.009
	w/w_n	.5000	1.1000	.800000	.2450852	.060
	E_s/E_c	.5000	2.0000	1.143333	.6230732	.388
	ρ_s/ρ_c	.8750	1.1250	.999167	.1046373	.011
Outputs	T_m/T_a	.0214	2.3059	.534276	.4362882	.190
	S_{1t}/S_{ta}	.0020	1.3893	.334517	.2991158	.089
	S_{1c}/S_{ca}	.0005	.0312	.007063	.0060265	.000
	S_{2t}/S_{ta}	.0000	.3505	.078145	.0744315	.006
	S_{2c}/S_{ca}	.0006	.0400	.010732	.0081236	.000
	S_{3t}/S_{ta}	.0000	.3482	.059655	.0676325	.005
	S_{3c}/S_{ca}	.0026	.1800	.044275	.0345279	.001
	Str/Str_u	.0015	.0940	.025049	.0193912	.000
	P_h/P_s	.0580	1.2912	.298081	.1964332	.039

The application of the SPSS software with the description above with many trials indicates that the best data subdivision is (79.7%) for training, (12.7%) for testing and (7.7%) for holdout (verification). The final network information, which involves input layer information (n = 12, scaling method is standardized), hidden layer(p = 16, activation function (F_h) is hyperbolic tanh) and output layer(m = 9, scaling method is standardized and activation function (F_0) is identity).

Figure (22) shows the architecture of the ANN model network prepared by SPSS software.

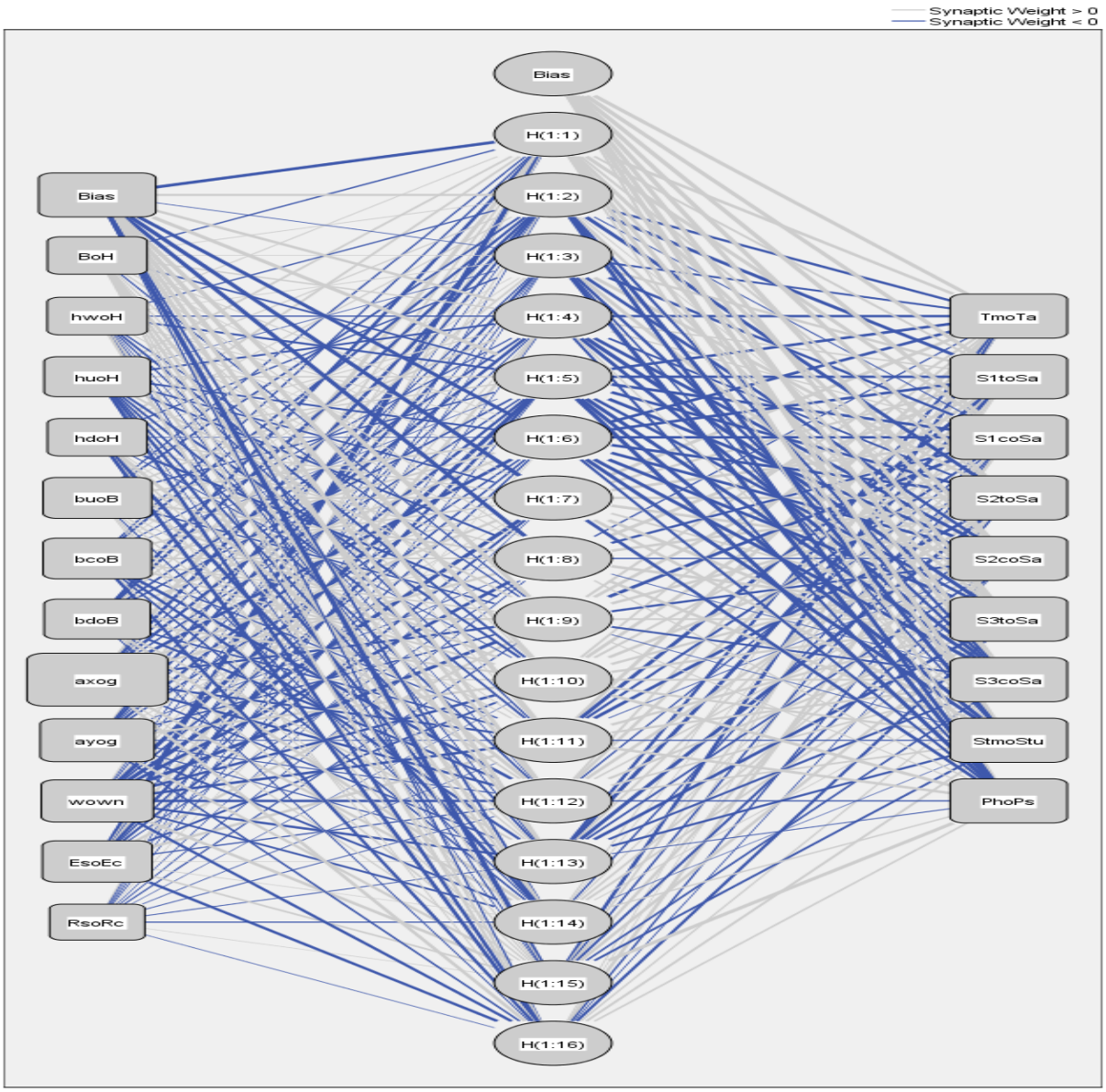

Fig. 22: Architecture of the ANN model network.

Table (6) shows the error analysis of the final weights matrices and bias vectors, selected by the software. The results indicate the lowest possible sum of square errors, for each subdivision and the relative error of each output variable in each subdivision. The most important ones are those of the holdout sub data, where the average overall error is low (0.014).

Tables (7) and (8) shows the outputs of SPSS software for the final weight matrices and the final bias vectors, which can be excreted to the following Equations:

$v_{o_{p\times 1}} = v_{o_{13\times 1}} = [Values\ in\ the\ first\ row\ of\ Table\ (7)]$

(23)$v_{n\times p} = v_{12\times 10} = [Values\ in\ the\ second\ to\ thirteenth\ row\ of\ Table\ (7)]$(24)

$w_{o_{m\times 1}} = w_{o_{9\times 1}} = [Values\ in\ the\ first\ row\ of\ Table\ (8)]$(25)

$w_{p\times m} = w_{10\times 9} = [Values\ in\ the\ second\ to\ seventeenth\ row\ of\ Table\ (8)]$ (26)

Table 6: Model summary.

Process	***Details***	***Dimensionless Variables***	***Values***
Training	Sum of Squares Error		44.830
	Average Overall Relative Error		.014
	Relative Error for Scale Dependents	T_m/T_a	.008
		S_{1t}/S_{ta}	.006
		S_{1c}/S_{ca}	.045
		S_{2t}/S_{ta}	.009
		S_{2c}/S_{ca}	.015
		S_{3t}/S_{ta}	.020
		S_{3c}/S_{ca}	.006
		Str/Str_u	.009
		P_h/P_s	.006
	Stopping Rule Used	Consecutive step(s) with no decrease in error*	
	Training Time	00:00:03.923	
Testing	Sum of Squares Error		7.418
	Average Overall Relative Error		.016
	Relative Error for Scale Dependents	T_m/T_a	.010
		S_{1t}/S_{ta}	.012
		S_{1c}/S_{ca}	.046
		S_{2t}/S_{ta}	.015
		S_{2c}/S_{ca}	.014
		S_{3t}/S_{ta}	.023
		S_{3c}/S_{ca}	.009
		Str/Str_u	.016
		P_h/P_s	.007
Holdout	Average Overall Relative Error		.014
	Relative Error for Scale Dependents	T_m/T_a	.009
		S_{1t}/S_{ta}	.010
		S_{1c}/S_{ca}	.027
		S_{2t}/S_{ta}	.010
		S_{2c}/S_{ca}	.018
		S_{3t}/S_{ta}	.019
		S_{3c}/S_{ca}	.007
		Str/Str_u	.013
		Ph/Ps	.011

**Error computations are based on the testing sample.*

Table 7: Input layer parameter estimates.

Predictor		Predicted															
		Hidden Layer 1															
		H(1:1)	H(1:2)	H(1:3)	H(1:4)	H(1:5)	H(1:6)	H(1:7)	H(1:8)	H(1:9)	H(1:10)	H(1:11)	H(1:12)	H(1:13)	H(1:14)	H(1:15)	H(1:16)
Input Layer	Biass	-2.688	.495	-.030	.652	3.190	-1.239	-2.891	-1.549	2.758	2.204	2.428	.826	1.023	-.177	-1.561	-.093
	B/H	-.121	.038	.014	.151	-.222	.067	.038	.083	-.090	.077	.068	.443	.330	.401	.116	.166
	h_w/H	.057	-.110	.041	-.133	-.397	.069	.025	.047	-.103	-.214	-.094	-.008	-.054	.268	-.070	.278
	h_u/H	.184	.081	-.025	-.319	.174	-.306	-.208	-.271	.211	-.281	-.195	-.159	-.162	-.315	-.012	-.404
	h_d/H	.199	.082	-.130	.093	.164	-.036	.160	.160	-.383	-.055	.051	.712	.129	-.572	.086	-.482
	b_u/B	-.102	-.174	.014	.221	-.161	.385	.334	.417	-.161	.434	.066	.157	.101	-.077	.104	.064
	b_c/B	-.108	-.251	.025	-.085	-.008	.298	.226	.259	.181	.324	-.121	-.528	-.341	-.140	.070	-.361
	b_d/B	-.425	-.380	.154	-.194	-.168	.310	.098	.046	.468	.418	-.202	-.369	.211	.476	.131	-.058
	a_x/g	.719	-.438	-.090	-.426	-.115	-.690	.465	.526	-.517	.134	-.473	-.525	-.161	.429	.085	.469
	a_y/g	.145	-.166	-.296	-.070	-.314	-.144	.044	-.038	-.161	.629	-.084	-.099	-.091	-.274	.382	-.139
	w/w_n	.061	-.019	-.032	.074	-1.321	-.147	-1.761	-.760	-1.676	-.576	-.947	-1.007	-.533	-.273	.677	-.430
	E_s/E_c	-1.857	.064	-.039	.339	-.402	-.116	-.218	-.063	.406	-.248	.709	-.115	.022	.015	.196	-.488
	ρ_s/ρ_c	.081	-.021	-.003	-.015	-.028	.008	-.004	-.041	-.086	.000	-.028	-.049	-.057	-.104	.006	-.018

Table 8: Hidden layer parameter estimates.

Predictor		***Predicted***								
		Output Layer								
		T_m/T_a	S_{1t}/S_{ta}	S_{1c}/S_{ca}	S_{1t}/S_{ta}	S_{1c}/S_{ca}	S_{1t}/S_{ta}	S_{1c}/S_{ca}	Str/Str_u	P_h/P_s
Hidden Layer	**(Biass)**	1.312	2.122	3.303	1.968	2.154	1.287	1.822	1.837	.234
	H(1:1)	.753	.245	1.069	.235	.874	.468	.925	.747	.139
	H(1:2)	-.502	-1.192	-.059	-.975	.046	.300	-.275	-.910	-.677
	H(1:3)	-.323	.655	-.478	.814	-.532	.671	-.339	-.138	-1.794
	H(1:4)	-.874	.182	.132	-.242	-.932	-1.500	-.785	.100	-.232
	H(1:5)	-1.183	-1.066	-1.791	-.930	-1.172	-.547	-1.139	-1.108	-1.289
	H(1:6)	-1.167	-1.302	-.957	-1.311	-1.143	-1.125	-1.173	-1.163	-.292
	H(1:7)	1.206	.468	1.202	.630	1.201	.291	1.087	.567	-.567
	H(1:8)	-.101	1.244	-.454	1.088	-.114	1.372	-.033	.760	.105
	H(1:9)	.280	.653	-1.227	.753	-.465	.296	-.336	-.029	.079
	H(1:10)	.180	.631	.293	.699	.520	.567	.399	.479	1.393
	H(1:11)	.601	-.860	-.282	-.689	-.030	.626	.475	-.127	.947
	H(1:12)	.187	.420	-.105	.467	.139	.326	.236	.275	-.136
	H(1:13)	-.330	-.814	.176	-.888	-.162	-.662	-.301	-.383	-.062
	H(1:14)	.064	.026	-.113	.073	.171	.177	.046	-.001	.139
	H(1:15)	-.435	.150	-.124	.298	-.220	.394	-.158	-.225	1.527
	H(1:16)	.048	.025	.389	-.114	-.027	-.311	.102	.225	.147

Figures (23) shows the comparison of the predicted and observed output variables, (T_m/T_a, S_{1t}/S_{ta}, S_{1c}/S_{ca}, S_{2t}/S_{ta}, S_{2c}/S_{ca}, S_{3t}/S_{ta}, S_{3c}/S_{ca}, $Str/Str_u$and P_h/P_s) respectively, with the correlation coefficients which are shown in Table (9).

Table 9: correlation between the predicted and observed output variables.

Variables	T_m/T_a	S_{1t}/S_{ta}	S_{1c}/S_{ca}	S_{2t}/S_{ta}	S_{2c}/S_{ca}	S_{3t}/S_{ta}	S_{3c}/S_{ca}	Str/Str_u	P_h/P_s
Correlation	0.996	0.996	0.978	0.995	0.992	0.990	0.997	0.995	0.997

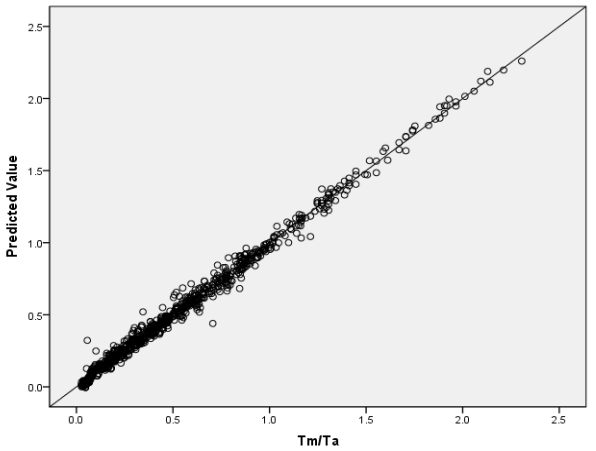
Predicted Value
Tm/Ta

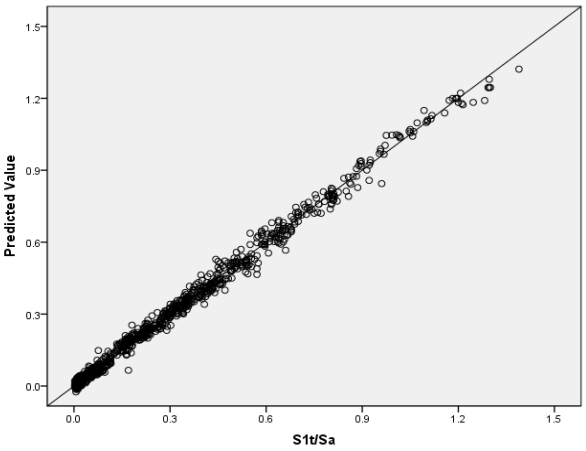
Predicted Value
S1t/Sa

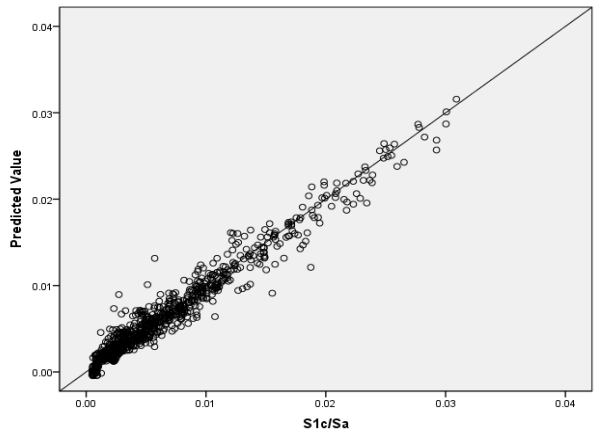
Predicted Value
S1c/Sa

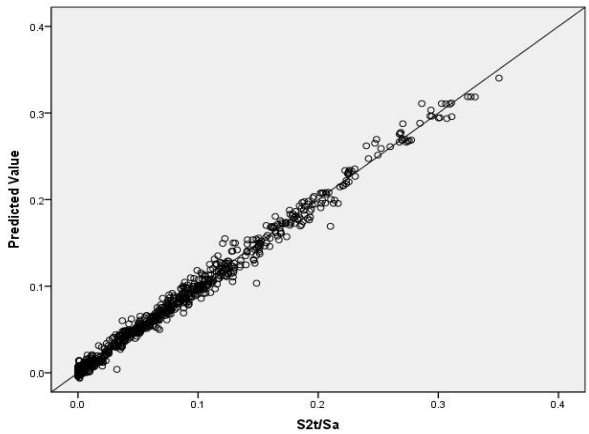
Predicted Value
S2t/Sa

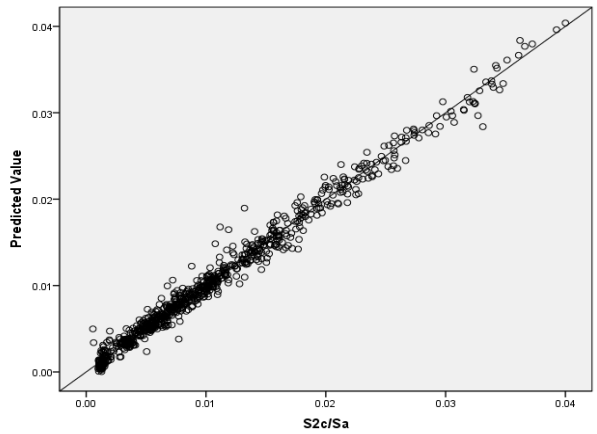
Predicted Value
S2c/Sa

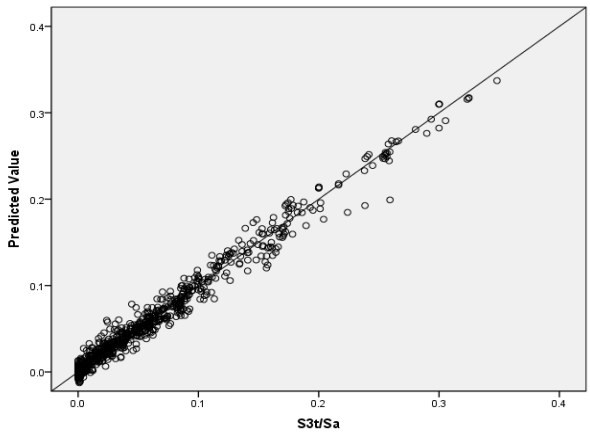
Predicted Value
S3t/Sa

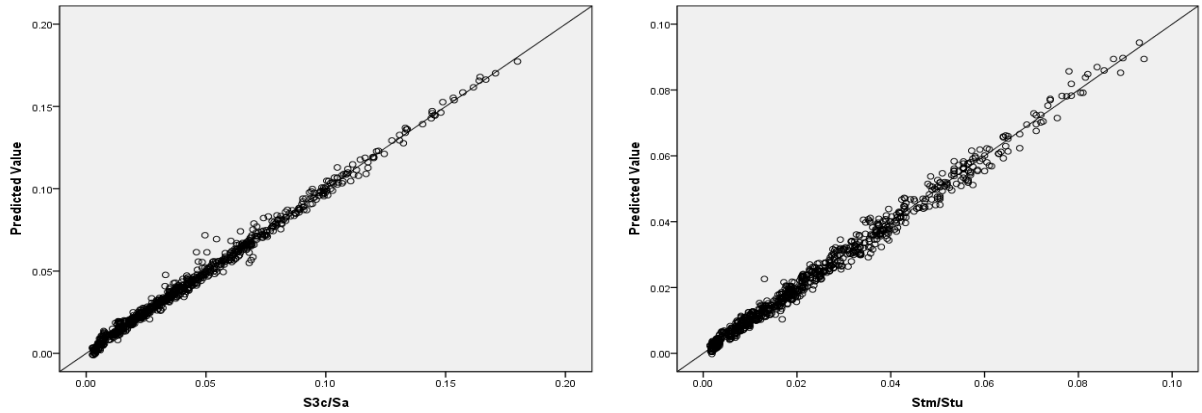

Fig. 23: Comparison of the predicted and observed variables.

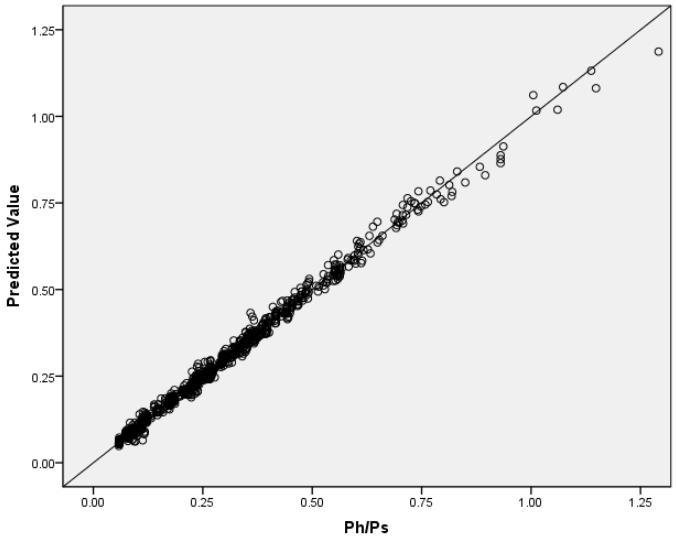

Fig. 23: Continued.

The SPSS software allows a normalized importance analysis to illustrate the relative effect of each input variable on the output variables. This analysis is shown in figure (24). It is obvious that the input variable sequence of effect on the output variables are (a_x/g, a_y/g,w/w_n, E_s/E_c,b_u/B, b_c/B, h_u/H, b_d/B, h_w/H, h_d/H, B/H and ρ_s/ρ_c) with (100%, 43.6%, 39.0%, 34.2%, 31.7%, 30.9%, 26.5%, 26.1%, 13.3%, 12.6%, 12.2% and 3.2%) respectively.

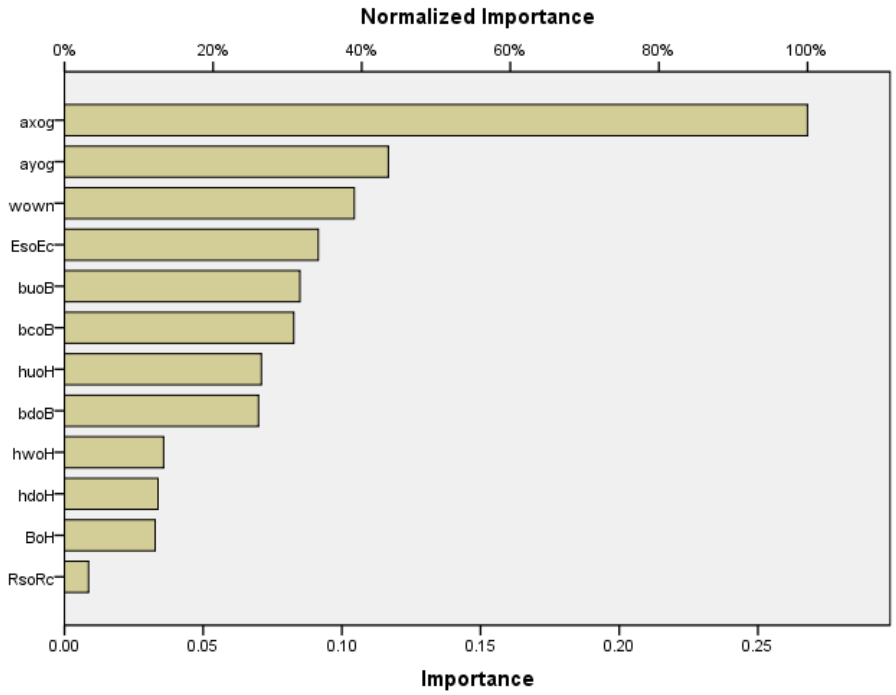

Fig. 24: Normalized importance for input variables.

Further Verification of the ANN Model

This is achieved here by selecting arbitrary three new cases with input data that not exist in the data base. However these input values are selected within the range of each one, but not exactly the values adopted in the data base. Table (10) shows the selected input variables for each of the three cases used.

Table 10: Input data for new three cases.

Input Variables	**B/H**	**h_w/H**	**h_u/H**	**h_d/H**	**b_u/B**	**b_c/B**	**b_d/B**	**a_x/g**	**a_y/g**	**w/w_n**	**E_s/E_c**	**ρ_s/ρ_c**
Case 1	0.84	0.92	0.62	0.88	0.08	0.13	0.79	0.25	0.00	0.80	1.00	1.00
Case 2	0.84	0.92	0.62	0.88	0.08	0.13	0.79	0.00	0.30	1.10	1.00	1.00
Case 3	0.84	0.92	0.62	0.88	0.08	0.13	0.79	0.15	0.20	0.50	1.00	1.00

Each case is analyzed using the ANSYS software to obtain the output results. The outputs of each case also are obtained using a MATLAB program. This program is written by using the developed ANN model with the estimated parameters shown in Table (5). These parameter include the values of the means and standard deviation for scaling and the obtained weight matrices and bias vectors given in Equations (24) and (26), with the activation functions obtained by the SPSS software, as hyperbolic tangent and identity for the hidden and output layers respectively.

Table (11) shows the results obtained from ANSYS software and the ANN model.

Table 11: Comparison of ANN model and ANSYS software results.

Variables	*Case 1*		*Case 2*		*Case 3*	
	ANSYS	*ANN*	*ANSYS*	*ANN*	*ANSYS*	*ANN*
T/T_a	0.7214	0.6758	0.2486	0.23198	0.9742	0.95316
S_{1t}/S_{ta}	0.5071	0.547	0.1544	0.13858	0.5643	0.6097
S_{1c}/S_{ca}	0.0070	0.00512	0.0113	0.01116	0.0108	0.00926

Variables	*Case 1*		*Case 2*		*Case 3*	
	ANSYS	*ANN*	*ANSYS*	*ANN*	*ANSYS*	*ANN*
S_{2t}/S_{ta}	0.1260	0.12847	0.0312	0.0283	0.1327	0.14041
S_{2c}/S_{ca}	0.0127	0.01137	0.0118	0.01084	0.0172	0.0168
S_{3t}/S_{ta}	0.1052	0.10856	0.02579	0.0236	0.1317	0.11063
S_{3c}/S_{ca}	0.0544	0.05242	0.0395	0.04128	0.0736	0.07249
Str/Str_u	0.0303	0.03511	0.0182	0.01746	0.0398	0.04458
P_h/P_s	0.2826	0.29472	0.7422	0.74386	0.3697	0.36183

Figures (25, 26 and 27) show the comparison between the results obtained from ANSYS software and the ANN model.

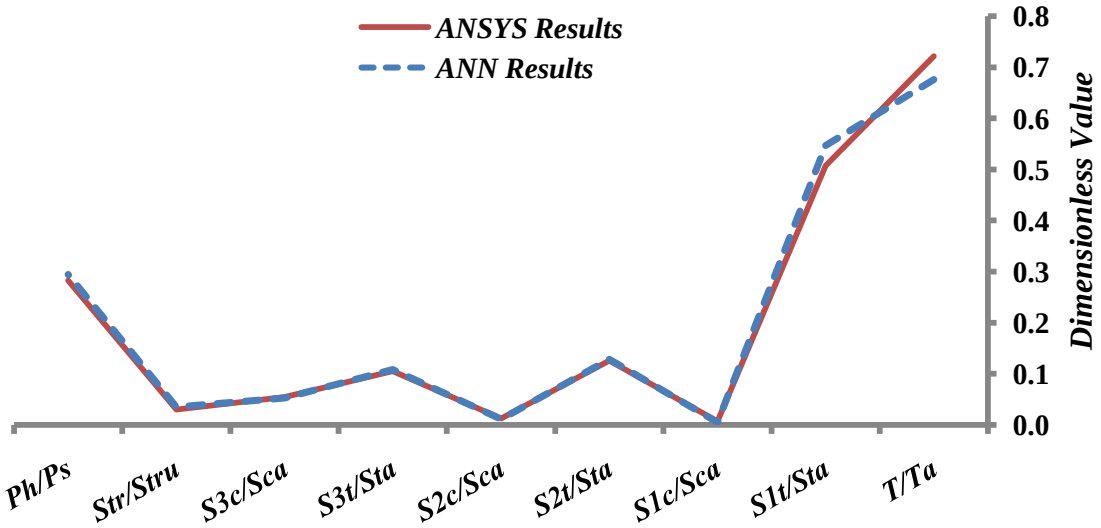

Fig. 25: Comparison of ANN model and ANSYS software results for case 1 (horizontal acceleration), correlation coefficient =0.996.

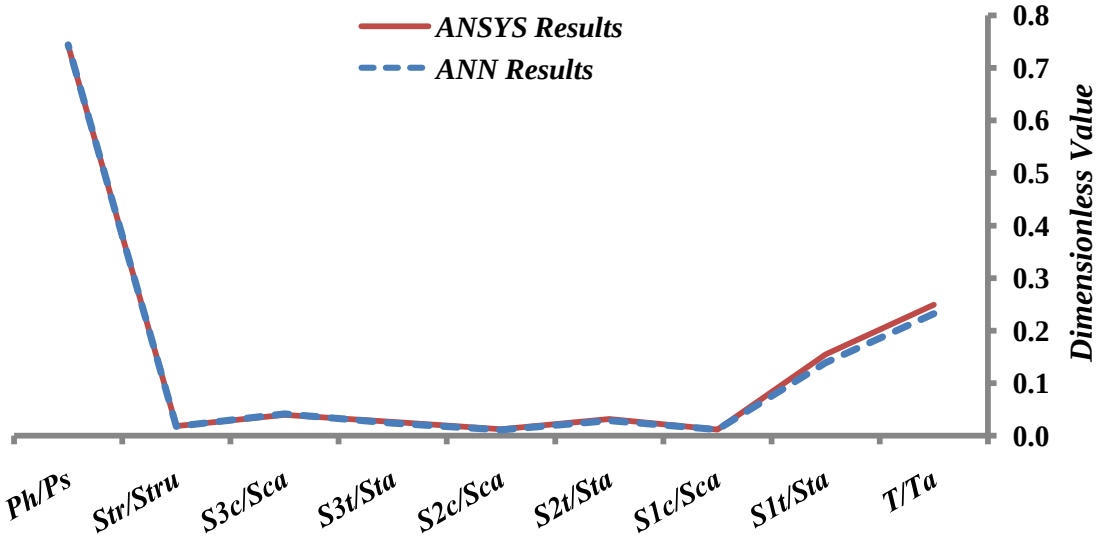

Fig. 26: Comparison of ANN model and ANSYS software results for case 2 (vertical acceleration), correlation coefficient =0.999.

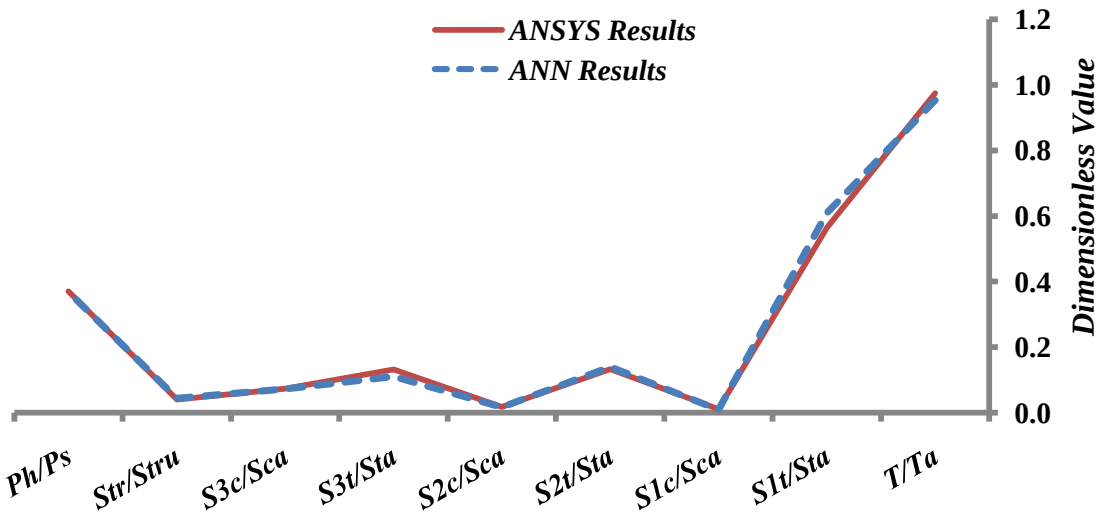

Fig. 27: Comparison of ANN model and ANSYS software results for case 3 (horizontal and vertical acceleration), correlation coefficient =0.998.

Conclusions

From the research conducted herein, the following conclusion can be deduced:

1- Results for the ANSYS analysis for the hydrodynamic dam- reservoir-foundation system indicates that the behavior of this system is different for the cases of horizontal earthquake acceleration only, vertical acceleration only and combined horizontal and vertical earthquake acceleration for a given geometrical dam section, given physical and mechanical properties of soil, concrete and water. These results necessitate the use of the known ranges of these properties to build a representative database to describe the behavior variation of the system. Hence many cases were used includes the variation of the independent variable such as earthquake accelerations amplitudes and frequencies, soil and concrete modulus of elasticity, densities, Poisson's ratios and geometrical dimensions of the dam section. Nine hundred cases were analyzed using ANSYS software was found to be an enough sample size for representation.

2- It was found that is necessary to divide the sample cases into three categories, one for horizontal acceleration only and one for the vertical acceleration and the last for combined horizontal and vertical accelerations.

3- The ANN modeling technique used for obtaining a model of direct estimation of the output variables (displacement, strain, shear stress, first principal stress, second principal stress, third principal stress and hydrodynamic pressure) for a given set of independent variables (horizontal acceleration, vertical acceleration, material properties and frequencies) was found to be capable to estimate the dependent variables accurately. The range of correlation coefficient of the dependent variables is (97.8% to 99.7%).

4- The required parameters of the ANN model to develop a reliable results are as follows; the data division into training, testing and holdout (verification) subsets is (79.7%, 12.7% and 7.7%) respectively. The minimum number of the hidden nodes in the hidden layer is sixteen (16). The average overall relative error is 1.4%, 1.6% and 1.4% for the training, testing and holdout subsets respectively. The optimum types of the activation functions of the hidden and output layer are hyperbolic tangent and identity functions respectively. The learning rate and momentum factor required are (0.4 and 0.9) respectively.

5- The comparison of the results of the ANN models for three cases selected in such a way that are not exist in the database used for building the ANN model with their corresponding results of these cases using ANSYS software, indicates the capability of this model to give very accurate results. The correlation coefficient in the three cases is 99.6% in the horizontal acceleration case, 99.9% in the vertical acceleration case and 99.8% in the dual acceleration (horizontal and vertical) case respectively.

Recommendations

For further research of this work, the following is recommended:

1- Applying the same technique adopted in this research to develop a model for earth dams.

2- Develop a similar model considering the non-homogeneity of the media, either for the soil

foundation only or for both soil foundation and concrete dam body.

3- Develop a similar model for gravity dam with galleries, silt and depression (fully or partially), and adding the bearing capacity of the soil as a restriction and must be checked.
4- Develop a similar model considering the effect of the reservoir surface wave generated due to seismic excitation and shape of the reservoir on the hydrodynamic pressure applied on the dam.
5- Use of radial base neural network modeling to developed the ANN model and compares its results with the developed back propagation ANN model to relate the input variables (geometrical and excitation variables) with the output variables stresses and strains.
6- Use the non-linear analysis to develop the ANN model for dams with initial cracks due to construction or ancient earthquakes.

References

[1.] Akkose M. &Simsek E., (2010), "Non-Linear Seismic Response of Concrete Gravity Dams to Near-Fault Ground Motions Including Dam-Water-Sediment-Foundation Interaction", Applied Mathematical Modeling, Volume 34, Issue 11, Pages 3685–3700.

[2.] Aviles J. & Suarez M., (2010), "Effects of Surface Waves on Hydrodynamic Pressures on Rigid Dams with Arbitrary Upstream Face", International Journal for Numerical Methods in Fluids, Volume 62, Pages 1155–1168.

[3.] Bayraktar A., TurkerT., Akkose M. &Ates S., (2010). "The Effect of Reservoir Length on Seismic Performanceof Gravity Dams to Near- and Far-Fault Ground Motions", Natural Hazards, Volume 52, Issue 2, Pages 257-275.

[4.] Béjar L. A., (2010), "Time-Domain Hydrodynamic Forces on Rigid Dams with Reservoir Bottom Absorption of Energy", Journal of Engineering Mechanics, ASCE, Volume 136, Issue 10, Pages 1271-1280.

[5.] Bouaanani N., Paultre P. &Proulx J., (2003), "A Closed-Form Formulation for Earthquake-Induced Hydrodynamic Pressure on Gravity Dams", Journal of Sound and Vibration, Volume 261, Issue 3, Pages 573–582.

[6.] Chopra A.K., (1967), "Hydrodynamic Pressures on Dams During Earthquakes", Journal of the Engineering Mechanics Division (ASCE) EM-6:93, Pages 205-223.

[7.] Chopra, A.K. & Charles, F.C., (1979), "Dynamic Method for Earthquake Resistant Design and Safety Evaluation of Concrete Gravity Dams", Proc., XIIIth Conference of the International Commission on large Dams, New Delhy, Pages 871-891.

[8.] Chwang A. T. &Housner J. W., (1978), "Hydrodynamic Pressures on Sloping Dams During Earthquakes. Part 1. Momentum Method" Journal of Fluid Mechanics, Volume 87, Part 1, Pages 335-341.

[9.] Fathi A. &Lotfi V., (2008), "Effects of Reservoir Length on Dynamic Analysis of Concrete Gravity Dams", The 14th World Conference on Earthquake Engineering(WCEE), Beijing.

[10.] Hacıefendioğlu K.,Bayraktar A. &Bilici Y., (2009), "The Effects of Ice Cover on Stochastic Response of Concrete Gravity Dams to Multi-Support Seismic Excitation", Cold Regions Science and Technology, Volume 55, Pages 295-303.

[11.] Heirany Z. &Ghaemian M., (2012), "The Effect of Foundation's Modulus of Elasticity on Concrete Gravity Dam's Behavior", Indian Journal of Science and Technology, Volume 5, Issue 5, Pages 2738-2740.

[12.] Karimi, N. KhajiK. N., M.T. Ahmadi M. T. &Mirzayee M., (2010),"System Identification of Concrete Gravity Dams Using Artificial Neural Networks Based on AHybrid Finite Element-Boundary Element Approach", Engineering Structures, Volume 32, Pages 3583-3591.

[13.] Khiavi M. P., (2011), "An Analytical Solution for Earthquake-Induced Hydrodynamic Pressure on Gravity Dams", World Academy of Science, Engineering and Technology, Volume 56.

[14.] Navayineya B., Amiri J. V. &Ardeshir M. A., (2009), "A Closed Form Solution for Hydrodynamic Pressure of Gravity Dams Reservoir With Effect of Viscosity Under Dynamic Loading", World Academy of Science, Engineering and Technology, Volume 58, Pages 416-420.

[15.] Novak P., Moffat A.I.B., Nalluri C. & Narayanan R., (2007), "Hydrodynamic Structures", Fourth Edition, Published by Taylor & Francis.

[16.] Olson L.G. & Bathe K.-J., (1983), "A Study of Displacement-Based Fluid Finite Elements for Calculating Frequencies of Fluid and Fluid–Structure Systems", Nuclear Engineering and Design, Volume 76, Issue 2, Pages 137–151.

[17.] Shariatmadar H. &Mirhaj A., (2009), "Modal Response of Dam-Reservoir-Foundation Interaction", 8th International Congress on Civil Engineering, Shiraz University, Shiraz, Iran.

[18.] U.S. Army Corps of Engineers, (1995), "Engineering and Design: Gravity Dam Design", Engineer Manual, Department of the Army, EM No. 1110-2-2200.
[19.] U.S. Army Corps of Engineers, (2003), "Engineering and Design: Time-History Dynamic Analysis of Concrete Hydraulic Structures", Engineer Manual, Department of the Army, EM No. 1110-2-6051.
[20.] Veltrop J.A., (2002), "Future of Dams", Journal of IEEE Power Engineering, Volume 22, Issue 3, Pages 12-15.
[21.] Victoria A. F., Herrera I. & Lozano C., (1969) "Hydrodynamic Pressures Generated by Vertical Earthquake Component", Fourth World Conference on Earthquake Engineering.
[22.] Westergaard H.M., (1933), "Water Pressures on Dams During Earthquakes", American Society of Civil Engineering, Trans. ASCE 98 Paper No. (1835), Pages 418–433.
[23.] Wikipedia, (2013), "Peak Ground Acceleration", The Free Encyclopedia, http://en.wikipedia.org/wiki/Peak_ground_acceleration.
[24.] Xie K.-Z., Meng F.-C., Zhang J.-S. & Zhou R.-Y., (2011), "Seismic Response Analysis of Concrete Arch Dam in Consideration of Water Compressibility", International Conference on Electric Technology and Civil Engineering (ICETCE), IEEE Catalog Number: CFP1102P-ART, ISBN: 978-1-4577-0290-7, Pages 6850-6853.
[25.] Yenigun, K. &Erkek, C., (2007), "Reliability in Dams and the Effects of Spillway Dimensions on Risk Levels", Journal of Water Resources Management, Volume 21, Issue 4, Pages 747-760.
[26.] Zienkiewicz O. C. & Taylor R. L., (2000), "The Finite Element Method", 5th Edition, Published by Butterworth-Heinemann, Volume 3: Fluid Dynamics, Oxford, UK.